Materials Today Chemistry 54 (2026) 103712

Contents lists available at ScienceDirect

Materials Today Chemistry

journal homepage: www.journals.elsevier.com/materials-today-chemistry/

An anionic PEGylated inulin-based carrier enables local pulmonary delivery of antibiotic colistin

Cinzia Scialabba [a], Nina Bono [b], Salvatore Emanuele Drago [a], Francesca Terracina [a], Paolo Tarsini [b], Emanuela Fabiola Craparo [a,*], Gabriele Candiani [b], Gennara Cavallaro [a]

[a] Lab of Biocompatible Polymers, Department of Biological, Chemical and Pharmaceutical Sciences and Technologies (STEBICEF), University of Palermo, Via Archirafi 32, Palermo, 90123, Italy
[b] GenT_LAB, Department of Chemistry, Materials and Chemical Engineering "G. Natta", Politecnico di Milano, Via Bassini 6, Milan, 20131, Italy

ARTICLE INFO

Keywords:
Colistin
Nanocomplex
Pulmonary delivery
Muco-diffusion
Gram-negative infections

ABSTRACT

Colistin (Col) is widely used to treat multidrug-resistant Gram-negative pulmonary infections, but its clinical efficacy is limited by poor mucus penetration, variable lung bioavailability, and systemic toxicity. This study developed an inulin (INU)-based graft copolymer as a nanocarrier to enhance pulmonary delivery, muco-diffusion, and controlled release of Col while preserving its antibacterial activity. INU was functionalized with a controllable substitution degree of succinic anhydride (SA) (DD_{Succ}: 27–197 mol%) to obtain an ionizable derivative with carboxyl groups in side chains. The derivative with a DD_{Succ} of 45 mol% was selected to graft 4 mol% of PEG chains, preserving ~40 mol% of ionizable carboxyl groups. The resulting copolymer (INU-Succ-PEG) was able to electrostatically complex Col (nanocomplexes of ~2 nm) and the aqueous dispersions showed excellent nebulization properties, with droplets <2 μm and a fine particle fraction >95%. Turbidimetric studies revealed reduced mucin interaction compared to free Col, enabling improved muco-diffusion. In vitro release studies demonstrated controlled drug release (<60% within 6 h), unaffected by mucin. The system showed good biocompatibility in bronchial cell lines. Antibacterial activity against *K. pneumoniae* and *E. coli* was preserved and superior to colistimethate sodium (CMS). Overall, the INU-Succ-PEG/Col system combines controlled release, high biocompatibility, improved mucus penetration, and optimal aerodynamic performance, representing a promising strategy for pulmonary treatment of chronic Gram-negative lung infections.

1. Introduction

Colistin (Col) is one of the most potent antibiotics available for treating infections caused by multidrug-resistant (MDR) Gram-negative bacteria [1]. Due to its unique mechanism of action targeting the outer membrane, Col retains activity against several clinically relevant pathogens that are frequently resistant to most other antimicrobial classes, including *Pseudomonas aeruginosa* (*P. aeruginosa)*, *Acinetobacter baumannii* (*A. baumannii)*, and *Klebsiella pneumoniae* (*K. pneumoniae*) [2].

Gram-negative bacteria represent a major global health threat because of their intrinsic resistance, remarkable genetic plasticity, and ability to rapidly acquire additional resistance determinants. In chronic infection settings, such as the lungs of patients with Cystic Fibrosis (CF), these pathogens can persist over long periods by adapting to the host environment, forming biofilms, and evading both immune responses and antibiotic treatment [2].

Due to significant systemic toxicity of colistin, including nephrotoxicity and neurotoxicity upon systemic administration, as well as bronchospasm and chest tightness when inhaled [3–5], Col is often used as a last-resort therapy for severe infections caused by MDR Gram-negative bacteria, and current market formulations utilize the prodrug colistin sodium methanesulfonate (colistimethate sodium, CMS) [6], generally administered by intravenous (IV) and/or inhalation as a dry powder or upon reconstituting the powder in sterile saline. However, the slow and highly variable conversion of CMS to active Col results in suboptimal and unpredictable concentrations in both lung and plasma. This leads to treatment inefficacy and promotes the development of bacterial resistance against the drug [6–9]. As a result, for the treatment of lung bacterial infections, both administration routes of CMS present significant challenges. IV may result in suboptimal drug concentrations in lung tissue, while inhalation therapy lacks standardization in dosing protocols. These limitations require the

* Corresponding author.
E-mail address: emanuela.craparo@unipa.it (E.F. Craparo).

https://doi.org/10.1016/j.mtchem.2026.103712
Received 23 March 2026; Received in revised form 11 May 2026; Accepted 14 May 2026
Available online 17 May 2026

implementation of rigorous monitoring strategies and adjustments based on patient condition, including regular assessment of creatinine clearance and plasma levels of the active drug, to optimize dosing based on individual patient response [1,7].

Moreover, several pieces of evidence emphasize the importance of using the active form of Col to achieve its effective bioavailability in lung tissue, reinforcing the need to prioritize this form in therapeutic strategies, especially for CF patients. These challenges have spurred extensive formulation research to address the variable outcomes associated with CMS treatment, aiming to reduce drug toxicity while improving lung bioavailability and antimicrobial activity. Some advances include the development of i) a polymeric prodrug of colistin sulphate [10]; ii) liposomal formulations for IV or as inhalable powders in combination with other antibiotics [11–13]; iii) inhalable lipid and polymeric nanoparticulate systems [14,15]; iv) aerosolizable Ivacaftor-loaded nanoparticles incorporated into colistin sulphate microparticles [16].

More recently, nanoparticles and micelles have been developed through electrostatic interactions of cationic Col with anionic polymers [17–19]. pH-responsive complexes composed of poly(β-amino ester) and hyaluronic acid (HA) were designed to release colistin preferentially in acidic microenvironments typical of infected tissues [17]. These systems demonstrated size modulation in response to pH changes and sustained antibiotic release, suggesting potential for improved local targeting and reduced systemic toxicity. Similarly, Dubashynskaya et al. investigated polyelectrolyte complexes between HA and Col, exploiting electrostatic interactions to generate nanoparticles with controlled release profiles and improved biocompatibility [18]. Coacervate core micelles exhibited high complexation efficiency, long-term stability, and drug protection from enzymatic degradation, without compromising their antibacterial activity [19]. Furthermore, the micelles maintained their structural integrity in the presence of serum proteins, highlighting their potential robustness for in vivo applications. Therefore, these recent strategies demonstrate the potential of polymeric nanoparticle-based delivery systems to improve Col therapy by enhancing targeted delivery, reducing toxicity, and overcoming challenges associated with biofilm-associated and multidrug-resistant infections.

For local lung therapies, developing dosage forms as powder-based and inhalable formulations offers two key advantages: it improves the drug's stability during storage by protecting it from chemical degradation, and it allows for direct delivery to the lungs, which reduces unwanted systemic effects throughout the body [20].

In this work, a negatively charged inulin-based graft copolymer (INU-Succ-PEG) was developed to form nanocomplexes with Col and improve its pulmonary delivery. Inulin (INU) was selected as a starting material to produce nanocarriers due to its favourable physicochemical and biological properties. It is a naturally derived, non-toxic, and biodegradable polysaccharide with a well-established safety profile and high biocompatibility [20,21]. Its structure, composed of flexible fructose chains and multiple hydroxyl groups, enables straightforward chemical modification and conjugation with various functional moieties, allowing the formation of stable nanocarriers under mild conditions [22–24]. In addition, inulin can provide steric stabilization at the nanoscale, reducing aggregation and enhancing the physical stability of the system [20]. A highly controllable and reproducible synthetic strategy was employed, enabling modulation of polymer charge while preserving favourable physicochemical properties such as aqueous solubility and limited polydispersity. Stable supramolecular nanocomplexes were successfully obtained through electrostatic interactions between the polymer and the drug. Advantageous aerodynamic properties after nebulization were observed, supporting efficient lung deposition. Reduced interaction with mucin and improved muco-diffusion compared to free Col were demonstrated, together with a controlled and sustained drug release profile. Preserved antibacterial activity and excellent biocompatibility toward bronchial epithelial cells were also confirmed. Overall, a promising nanotechnological platform for the treatment of chronic Gram-negative pulmonary infections was established, offering improved local delivery and exposure control compared to Col alone.

2. Materials and methods

2.1. Materials

All reagents used were of analytical grade. The following materials were purchased from Sigma Aldrich (Italy): inulin (INU) extracted from *Dahlia* tubers (M_r ~5000), 4-dimethylaminopyridine (DMAP), anhydrous N,N-dimethylformamide (DMF-a), succinic anhydride (SA), N-(3-dimethylaminopropyl)-N′-ethylcarbodiimide hydrochloride (EDC), N-hydroxysulfosuccinimide (NHSS), methoxypolyethylene glycol amine (CH_3O-PEG_{2000}-NH_2), colistimethate sodium (CMS), ampicillin, phosphate-buffered saline (PBS), sodium chloride (NaCl), sodium sulphate (Na_2SO_4), HPLC-grade acetonitrile (ACN), acetone, diethyl ether, and mucin extracted from porcine stomach. Colistin sulphate was purchased from Cayman Chemical Company (USA). Dialysis membranes were purchased from Spectrum Labs (USA). The human bronchial epithelial cell line 16HBE was obtained from the Istituto Zooprofilattico Sperimentale della Lombardia (Brescia, Italy), while the BEAS cell line was purchased from Clini-Sciences (Guidonia Montecelio, Italy).

^{1}H NMR spectra were recorded using a Bruker Avance II-300 spectrometer (300 MHz).

The weight-average molecular weights ($\overline{M}_w$) of INU, INU-Succ, and INU-Succ-PEG were determined by size exclusion chromatography (SEC). The system consisted of a pump and a PolySep-GFP P4000 column (Phenomenex) connected to an Agilent 1260 Infinity Multi-Detector GPC/SEC equipped with a refractive index detector. The mobile phase was 0.15 M citrate/phosphate buffer at pH 5.5, and flow rate was 0.8 mL/min; the column temperature was kept at 25 °C. Each sample (15 mg/mL) was dissolved in the mobile phase and filtered through a 0.2 μm cellulose acetate syringe filter. The calibration curve was obtained using polyethylene glycol standards (1–25 kDa).

2.2. Synthesis of INU-Succinate (INU-Succ)

INU-Succ was synthesized by dispersing INU (500 mg, 3.086 mmol of repeating units) in 5 mL of DMF-a, followed by the addition of DMAP (74.5 mg, 0.61 mmol). After 10 min, SA (154.4 mg, 1.543 mmol) was added. The reaction was carried out in a microwave reactor (CEM Discover Microwave Reactor) under 25 W irradiation for 1 h, maintaining the temperature at ~ 60 °C by external cooling with compressed air [25]. Then, the reaction mixture was precipitated in excess diethyl ether, and the solid product was recovered by centrifugation at 9000 rpm for 5 min at 4 °C. The precipitate was washed three times with acetone, and the obtained product was purified by exhaustive dialysis using a membrane with nominal molecular weight cut-off (MWCO) of 1 kDa against saturated NaCl solution for 2 days, followed by distilled water for 3 days. The purified dispersion was then freeze-dried to yield INU-Succ (75 wt%). The reaction was repeated at least three times. The stoichiometric mole ratios were: DMAP/INU repeating units = 0.2 and SA/INU repeating units = 0.5.

The polymer was characterized by ^{1}H NMR (300 MHz, D_2O), which showed the following peaks: δ 2.64 and 2.70 ($4H_{Succ}$ -C**H$_2$**C**H$_2$**COOH), δ 3.5–4.0 ($5H_{INU}$ -C**H$_2$**OH; -C**H**CH_2OH; -CC**H$_2$**O-), 4.12 ($1H_{INU}$, -C**H**OH), 4.28 ($1H_{INU}$, -C**H**OH).

2.3. Synthesis of INU-Succ-PEG

The functionalization of INU-Succ with $CH_3OPEG_{2000}NH_2$ was performed in an aqueous phosphate buffer solution, using EDC·HCl and NHSS as activating agents, according to the following stoichiometric conditions: mole ratios between EDC/INU-Succ units = 0.1 and NHSS/

INU-Succ units = 0.1. To a dispersion of INU-Succ (250 mg, 1.2 mmol repeating units) in 4 mL of bidistilled water, a proper amount of NHSS (26 mg, 0.12 mmol) and EDC·HCl (23 mg, 0.115 mmol) were added. The pH was adjusted to 6.8 using 0.1 N NaOH, and the mixture was stirred at room temperature (rt) for 2 h. Subsequently, 4 mL of a PEG dispersion (170 mg in PBS, pH 7.4) was added dropwise and the mixture was stirred overnight at rt, using a stoichiometric mole ratio between PEG/INU-Succ units = 0.07. The product was purified by exhaustive dialysis (MWCO 1 kDa) against distilled water acidified to pH 5.5 with 1 N HCl. The final product was recovered by freeze-drying, and the yield was found to be equal to 80 wt% compared to the starting INU-Succ. The reaction was repeated at least three times.

The ^{1}H NMR spectrum in D_2O (300 MHz) showed the following peaks: δ 2.64 and 2.70 ($4H_{Succ}$ -C**H**$_2$C**H**$_2$COOH), δ 3.5–4.0 ($5H_{INU}$, -C**H**$_2$OH; -C**H**CH$_2$OH; -CC**H**$_2$O-), δ 3.7 ($4H_{PEG}$ -[C**H**$_2$C**H**$_2$O]$_{44}$-), 4.12 ($1H_{INU}$, -C**H**OH), 4.28 ($1H_{INU}$, -C**H**OH).

2.4. Potentiometric titration

A 25 mL sample of INU-Succ, INU-Succ-PEG and INU (1 mg/mL) was titrated under an argon atmosphere with 0.066 N NaOH until reaching pH 11. To stabilize the ionic strength, the samples were dispersed in a degassed 0.1 N NaCl aqueous solution. Prior to performing the potentiometric titrations, a Jenway differential electrometer was calibrated using a set of standard buffer solutions ($2.50 \pm 0.01 < pH < 10.00 \pm 0.01$). The titration was repeated three times.

2.5. Preparation of INU-Succ-PEG/Col nanocomplexes

A dispersion of INU-Succ-PEG (50 mg in 18 mL PBS, pH 6.5) was gently added, under continuous stirring, to a solution of colistin sulphate (Col) (15 mg in 2 mL PBS, pH 6.5) to achieve a COO^- (polymer)/NH_3^+ (Col) charge ratio of 1. The resulting mixture was transferred into a regenerated cellulose dialysis membrane (MWCO 1 kDa) and dialyzed against distilled water for 24 h with periodic replacement of the medium.

The purified dispersion was then filtered through a 5 μm regenerated cellulose (RC) syringe filter to remove residual aggregates, frozen in liquid nitrogen, and freeze-dried. The nanocomplexes were recovered with a yield of 69 ± 2.3 % and stored for further characterization. The complexation was repeated at least six times.

2.6. Characterization of INU-Succ-PEG/Col nanocomplexes

2.6.1. Drug loading (DL%)

Drug loading was quantified by high-performance liquid chromatography (HPLC) using an Agilent 1260 Infinity II system equipped with an autosampler (100 μL injection volume), a UV–Vis detector (set at λ = 214 nm), and a C18 column (250 × 4.6 mm). The mobile phase consisted of ACN/Na_2SO_4 buffer 0.03 M at pH 2.5 (25:75 v/v), operating with a flow of 1 mL/min. The analysis was performed in isocratic conditions at 25 °C, and Col was detected at λ = 215 nm. Samples were prepared by dispersing a known quantity of INU-Succ-PEG/Col nanocomplexes in the mobile phase and filtered using 0.22 μm RC syringe filters. The amount of loaded drug into the nanocomplexes, expressed as drug loading % (DL%), was calculated using a calibration curve obtained from different concentrations of Col. The analysis was repeated at least six times.

2.6.2. In vitro release studies

Release studies were performed in two different release media: PBS (pH 7.4) and simulated lung fluid (SLF, type 4) [26]. Nanocomplexes corresponding to 2.5 mg of Col were dispersed in 3 mL of proper medium, filtered by a 0.22 μm RC syringe filter, and transferred into a dialysis membrane tube (MWCO 1 kDa). Each dialysis membrane was immersed in 27 mL of the same medium and incubated in an orbital shaker at 37 °C under continuous stirring (100 rpm). At predetermined intervals, aliquots of 1 mL were withdrawn and replaced with an equivalent volume of fresh medium. Each collected medium was filtered through a 0.22 μm RC syringe filter and analysed by HPLC under the previously described conditions. Free Col diffusion was used as a control. Release studies in PBS (pH 7.4) were also conducted by placing inside the dialysis membrane, together with the nanocomplex or with the free Col used as the control, a mucin dispersion (1 mg/mL), following the same procedures described above. All experiments were performed in triplicate.

2.6.3. Critical aggregation concentration (CAC)

The critical aggregation concentration (CAC) was determined by pyrene fluorescence assay [27]. A stock solution of pyrene (6.0×10^{-5} M in acetone) was prepared, and 20 μL aliquots were transferred into vials and allowed to evaporate at 37 °C. Subsequently, 2 mL of aqueous dispersions of Col and INU-Succ-PEG/Col nanocomplexes, at Col concentrations corresponding to 15 to 0.00001 mg/mL, were added to obtain a final pyrene concentration of 6.0×10^{-7} M. Samples were incubated for 24 h at 37 °C under continuous shaking to allow equilibration, and fluorescence emission spectra were recorded at 25 °C using an λ_{ex} = 333 nm, collecting emission between 340 and 450 nm. The CAC was determined by plotting the intensity ratio of the first and third vibronic bands of pyrene (I373/I384) as a function of the logarithm of the sample concentration. This ratio reflects changes in the polarity of the microenvironment surrounding pyrene and is commonly used to detect the onset of aggregation. The CAC was taken from the intersection of the tangent to the curve at the inflection with the tangent of the horizontal tract of the curve. Each experiment was performed in triplicate.

2.6.4. Atomic force microscopy (AFM)

AFM micrographs were obtained using a FAST-SCAN microscope equipped with a closed-loop scanner (X, Y, and Z maximum scan regions: 35, 35, and 3 μm, respectively). Analysis was performed in soft tapping mode using a probe with an apical radius of 5 nm operating at 1400 kHz (k: 18 N/m). Freshly prepared nanocomplexes were diluted 1:100 in bidistilled water and deposited onto freshly cleaved mica substrates before analysis.

2.6.5. Turbidimetric analysis

The interaction between nanocomplexes and mucins, as well as between free Col and mucins, was evaluated by a turbidimetric assay. A 100 μL aliquot of nanocomplex dispersion or free Col solution, at a concentration corresponding to 0.2 mg/mL of Col, was mixed 1:1 (v/v) with 100 μL of mucin dispersion (2 mg/mL) and incubated at 37 °C under shaking. Turbidity was monitored by measuring the absorbance at λ = 500 nm at predetermined time points (0, 0.5, 1, 2, 3, and 4 h). In parallel, absorbance of the nanocomplex dispersion or free Col solution in water at λ = 500 nm was recorded, to subtract the background scattering attributable to the polymer or drug. Results were expressed as percentage transmittance relative to mucin, calculated as: (T_{500}sample/T_{500} mucin) × 100. All experiments were performed in triplicate.

2.6.6. Mucodiffusion

The diffusion behaviour of the nanocomplex through the CF-AM layer was evaluated using vertical Franz diffusion cells. Cystic fibrosis artificial mucus (CF-AM) was prepared according to a modified formulation designed to mimic the physicochemical properties of pathological sputum. Briefly, 50 mg of DNA, 25 mg of mucin from porcine stomach (Type II), 0.0295 mg of DTPA, 0.1 mL of RPMI 1640 amino acid solution, 25 μL of egg yolk emulsion, 25 mg of NaCl, and 11 mg of KCl were dissolved in DNase-free water to a final volume of 5 mL. The mixture was stirred continuously at room temperature until complete homogenization and then stored at 4 °C until use [28].

A filter paper membrane (pore size 0.45 μm) was used between the donor and acceptor compartments. The acceptor compartment contained 5 mL of DPBS buffer (pH 7.4), while the donor compartment was loaded with 200 μL of CF-AM, followed by the addition of 1 mL of either free Col solution (2 mg/mL) or the nanocomplex, in an amount corresponding to the free drug. The systems were incubated at 37 °C, and sampling was conducted by withdrawing 200 μL of solution at scheduled time intervals (1h, 2h, 3h, 4h, 5h, 6h, and 24h) and replacing it with the same volume of fresh medium. All samples were analysed by HPLC under the previously described conditions to quantify the amount of diffused drug. Each experiment was performed in triplicate, and results are reported as mean ± standard deviation (SD).

2.6.7. In vitro pulmonary drug deposition

The aerosolization performance of the nanocomplexes was evaluated using an Andersen Cascade Impactor (ACI) (InPharmaTEC, Cogliate (MB), Italy) [28]. Before use, the ACI was refrigerated at 4 °C for 2 h to minimize evaporation of nebulization droplets, which could otherwise reduce droplet size and alter deposition behaviour. Aerosolization was carried out using an air-jet nebulizer connected to a mouthpiece, positioned at the ACI inlet through a dedicated adapter. The system was then connected to a vacuum pump (Bavo X BIO, TCR TECORA®, Italy). For each nebulization experiment, 2.5 mL of the nanocomplex aqueous dispersion was filtered by a 0.22 μm RC syringe filter and loaded into the nebulizer chamber. Nebulization was performed for 15 min using the ACI setup operating at a flow rate of 29 L/min. The corresponding aerodynamic cut-off diameters were as follows: stage 0 (9 μm), stage 1 (5.8 μm), stage 2 (4.7 μm), stage 3 (3.3 μm), stage 4 (2.1 μm), stage 5 (1.1 μm), stage 6 (0.7 μm), stage 7 (0.4 μm). The pump flow was set to 4.5 L/min to ensure proper distribution of the aerosol fractions across the impactor stages. After nebulization, the nanocomplexes deposited on each stage were recovered using 1 mL of Na_2SO_4 solution at pH 2.5 (the aqueous component of the mobile phase used for HPLC analysis). The collected samples were analysed by HPLC under the conditions described previously. Free drug nebulization, used as a control, was performed under the same experimental conditions. All experiments were carried out in triplicate. HPLC data were used to calculate the fine particle fraction (FPF%), defined as the percentage of the emitted dose with an aerodynamic diameter below 5.0 μm, the mass median aerodynamic diameter (MMAD), and geometric standard deviation (GSD).

2.7. In vitro characterization of INU-Succ-PEG/Col nanocomplexes

2.7.1. Cell viability

Cytotoxicity of INU-Succ-PEG/Col nanocomplexes was evaluated on two human bronchial epithelial cell lines (16 HBE and BEAS) by MTS assay, using a commercially available kit Cell Titer 96 ® Aqueous one Solution cell proliferation assay (Promega, Milan, Italy). 16HBE and BEAS cells were seeded in 96-well plates at a density of 2×10^4 cells/well. Once confluent, cells were incubated with culture medium containing nanocomplexes, INU-Succ-PEG, and free Col at drug equivalent concentrations ranging from 8 to 256 μg/mL, filtered by a 0.22 μm RC syringe filter prior to use. After 24 and 48 h of incubation, the wells were washed twice with DPBS, and 100 μL of DMEM supplemented with 20 μL of MTS reagent was added. Plates were incubated for 2 h at 37 °C, and absorbance was measured at 492 nm. Cell viability was expressed as the percentage of absorbance relative to untreated control cells.

2.7.2. Antibacterial tests

The antibacterial effectiveness of Col derivatives was evaluated according to the ISO 20776-1:2020 standard. Tests were conducted against two Gram-negative bacterial strains: *Escherichia coli* (*E. coli* JM109 strain) and *Klebsiella pneumoniae* (*K. pneumoniae*). Bacteria were cultured in 5 mL of Luria-Bertani (LB) broth at 37 °C with shaking at 130 rpm overnight until reaching an optical density at $\lambda = 600$ nm (OD_{600}) of approximately 1, corresponding to ~10^9 bacteria/mL. Bacterial suspensions were subsequently diluted in standardized Mueller-Hinton broth (MHB) to a final concentration of ~10^6 bacteria/mL (referred to as the bacterial test inoculum for experiments).

For antibacterial testing, 50 μL/well of the bacterial test inoculum was transferred to separate wells of 96-well plates, followed by the addition of 50 μL/well of MHB broth containing the nanocomplexes. Plates were then incubated at 37 °C for 24 h. Bacteria inoculated in 50 μL/well of LB served as positive controls (CTRL+) for bacterial growth [29], while bacteria inoculated in 50 μL/well of Col and colistimethate sodium (CMS) solutions, INU-Succ-PEG/Col nanocomplex and INU-Succ-PEG copolymer aqueous dispersions (filtered by a 0.22 μm RC syringe filter prior to use) and ampicillin solution (at different concentrations) were used as internal references. The antibacterial efficacy of each compound was evaluated using the turbidity method (i.e., OD_{600} measurements) as previously reported [30]. After 24 h post-inoculation, the OD_{600} of each well (n = 3 per molecule) was measured using a GENios microplate reader (Tecan, Italy). The minimum inhibitory concentration (MIC) was calculated as the lowest concentration of each compound that reduced the optical density of the inoculum by 100% within 24 h of incubation compared to the CTRL + [31]. The bacterial reduction was calculated according to the following equation: Antibacterial reduction [%] = $(1 - OD_{600nm}\ \text{compound}/OD_{600nm}\ \text{CTRL+}) \times 100$.

2.8. Statistical analysis

Unless otherwise indicated, the results are presented as the mean ± standard deviation (SD) of a minimum of three independent measures. Comparisons between two groups were conducted using the independent samples *t*-test. A p-value of less than 0.05 was considered statistically significant.

3. Result and discussion

3.1. Synthesis and characterizations of inulin (INU)–based copolymers

A new negatively charged Inulin (INU)-based graft copolymer was synthesized with the aim of producing a polymeric nanocarrier capable of efficiently complexing and delivering colistin (Col) to the lower respiratory tract for the local treatment of pulmonary infections. INU, selected as the starting polymer, is a natural, highly biocompatible polysaccharide whose non-cytotoxic, non-haemolytic, and non-immunogenic features, together with its excellent water solubility, have made it a well-established biomaterial for drug-delivery applications [25,28,32].

In the first step of the synthetic process, INU was functionalized with succinic anhydride (SA) to introduce ionizable carboxyl groups along the polysaccharide backbone, conferring a negative charge at physiological pH and providing reactive handles for subsequent derivatization [33]. The esterification between INU hydroxyl groups and the carboxyl functionalities generated upon SA ring opening was performed in a microwave reactor under controlled temperature and power conditions, which significantly shortened reaction times and ensured high derivatization efficiency, in line with previous reports on microwave-assisted polysaccharide chemistry [34,35]. The schematic reaction is illustrated in Fig. 1A (step a).

Being the mean values of DD characterized by low standard deviation, obtained by repeating the reaction at least three times, the succinylation reaction proved to be highly reproducible and efficient; by modulating the molar ratio between SA and the INU repeating units from 0.3 to 2, in fact, copolymers with correspondent degrees of substitution were obtained (Fig. 1; $y = 0.9807x$, $R^2 = 0.9996$), thus enabling precise control over the number of introduced carboxyl groups and the resulting charge density of the INU-Succ samples.

The degree of derivatization (DD_{Succ}%) of INU-Succ was determined by ^1H NMR analysis (see spectrum in Fig. 1B), comparing the integrals of

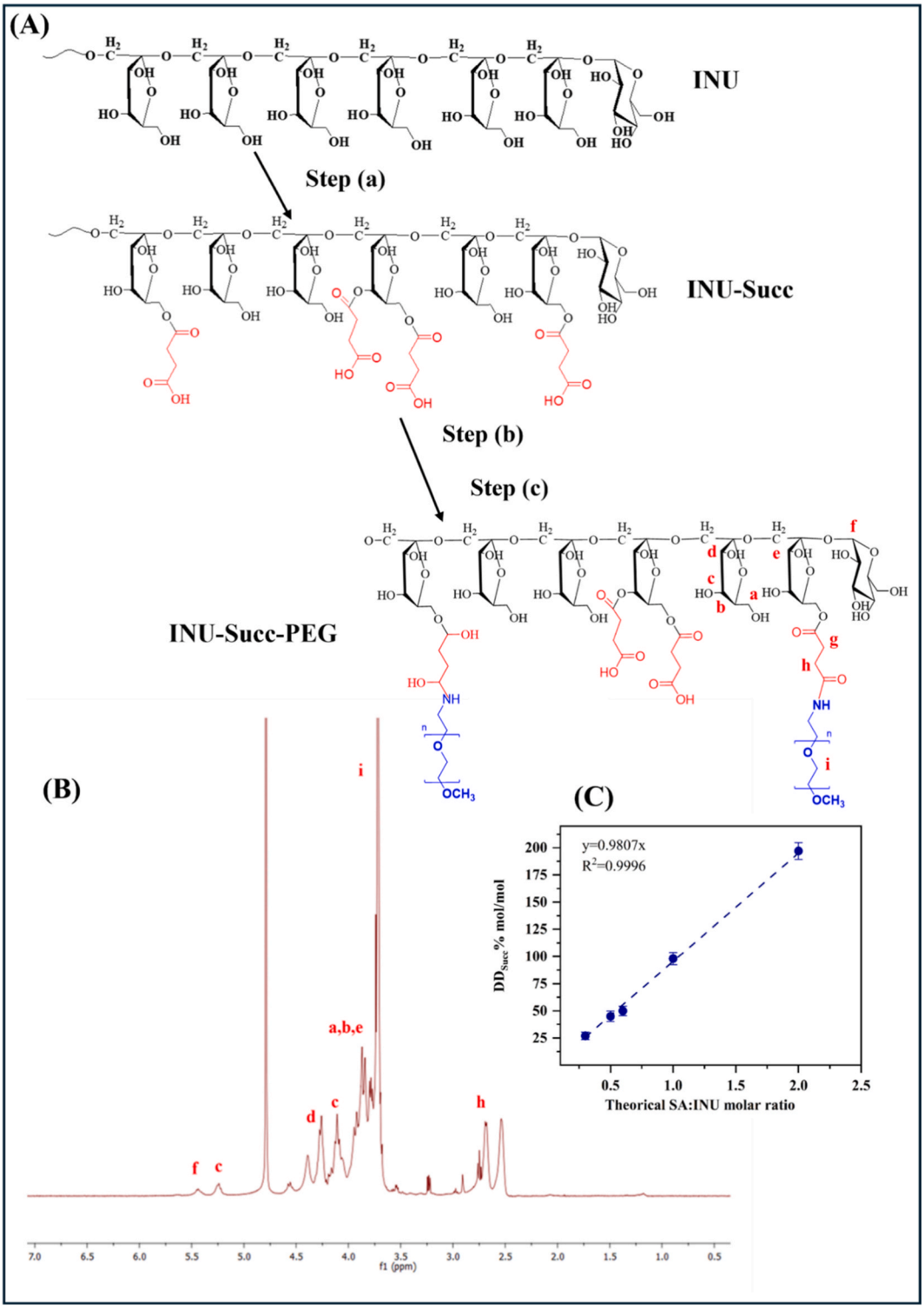

Fig. 1. (A) Schematic representation of the INU-Succ-PEG synthesis: (a) DMFa, SA, DMAP, 1h, 60 °C, 25 Watt; (b) EDC/NHSS, 2h PBS pH 6.5; (c) CH_3O-PEG-NH_2, PBS pH 7.4, 18h, 25 °C (n = 44); (B) The ^{1}H NMR spectrum of INU-Succ-PEG in D_2O; (C) trend of experimental vs theoretical molar ratio of SA:INU repeating units, calculated from ^{1}H NMR spectra.

the signals at δ 2.64 and 2.70 assigned to the succinate moieties ($4H_{succ}$ -CH_2CH_2COOH), with those of the INU units at 4.12 ($1H_{INU}$, -CH_2OH) and 4.28 ($1H_{INU}$, -CH_2OH). As shown in Fig. 1C, the experimental DD_{Succ}% increased in a controlled and predictable manner as the SA:INU molar ratio was raised. At low ratios (SA:INU = 0.3–0.6), the resulting DD_{Succ} values ranged from 27 % to 59 %, confirming that the introduction of carboxyl functionalities can be finely modulated. Increasing the theoretical molar ratio to 1.0 led to an almost quantitative conversion (DD ≈ 98 %), whereas using an excess of SA (molar ratio = 2.0) enabled the incorporation of nearly two succinyl groups per INU repeating unit (DD_{Succ} ≈ 197 %). Moreover, the low standard deviation obtained from the functionalization values by repeating the reaction at least three times further confirm the excellent reproducibility of the process. Overall, these results demonstrate that the succinylation

reaction provides a robust and tunable platform for obtaining INU-Succ derivatives with precisely adjustable charge densities across a broad substitution range. All derivatives were obtained in high yield ranging between 75 and 85 wt%.

The INU-Succ derivative with a DD_{Succ} of 45 ± 2 mol% relative to INU repeating units, corresponding to approximately ten carboxylic groups per polymer chain, was chosen for further functionalization with CH_3O-PEG-NH_2 to enhance the hydrophilicity of the system and impart stealth characteristics [36]. The terminal amine of PEG effectively reacted with a fraction of the residual carboxyl groups on INU-Succ via a carbodiimide-mediated coupling, giving the graft copolymer INU-Succ-PEG in good yield, as illustrated in Fig. 1 (step b-c). The degree of PEG derivatization (DD_{PEG}%) was quantified by ^{1}H NMR analysis, comparing the integral of the PEG protons at δ 3.7 ($4H_{PEG}$ -[CH_2CH_2O]$_{44}$-), with those of INU at 4.12 ($1H_{INU}$, -CH_2OH) and 4.28 ($1H_{INU}$, -CH_2OH), resulting equal to 4 ± 0.5 mol%. The weight-average molecular weight ($\overline{M}_w$), number-average molecular weight ($\overline{M}_n$), and polydispersity ($\overline{M}_w/\overline{M}_n$), determined by SEC as described in the Experimental Section, are reported in Table 1.

As expected, both INU-Succ and INU-Succ-PEG exhibited higher $\overline{M}_w$ and $\overline{M}_n$ values than the starting INU (5000 Da), while the polydispersity remained low, confirming successful controlled succinylation and pegylation, respectively, as well as a uniform molecular weight distribution. The INU-Succ-PEG derivative with a DD_{Succ} and DD_{PEG} of 45 mol % and 4 mol%, respectively, was selected as a compromise between sufficient carboxyl group density for effective functionalization, preservation of copolymer solubility and structural integrity of INU, and to ensure an appropriate balance between steric stabilization and maintenance of the system's physicochemical properties, avoiding excessive shielding that could hinder interactions.

While the PEG chains play a key role as solubilizing moieties, improving the aqueous stability of the resulting nanocomplexes, the ionization state of the acidic moieties on the copolymer backbone governs the strength and stability of the electrostatic complexation with amine groups of the drug. Therefore, the acid–base behaviour of INU-Succ-PEG was investigated by determining the pKa by potentiometric titration, which was found to be 5.2 (Fig. 2), consistent with the presence of succinate carboxyl groups that retain their dissociation capability even after PEG conjugation. Moreover, a comparison of the titration curves of INU, INU-Succ, and INU-Succ-PEG revealed that the PEGylated copolymer reached the equivalence point with a lower volume of titrant, as expected, reflecting a reduction in free carboxyl groups due to their functionalization with PEG.

3.2. Production and characterization of INU-Succ-PEG/Col nanocomplexes

Following its physicochemical characterization, INU-Succ-PEG was employed to form polyelectrolyte nanocomplexes with Col (INU-Succ-PEG/Col), exploiting complementary electrostatic interactions between the anionic carboxylate groups of the copolymer and the protonated amine groups of Col. Considering that each polymer chain bears approximately ten ionizable carboxylic groups and each Col molecule contains five protonable amines, the system provides a favourable multivalent ionic framework for stable complex formation. The resulting nanocomplexes exhibited a drug loading (DL%) of 22 ± 1.9 % (w/w)

Table 1
Weight-average molecular weight ($\overline{M}_w$), number-average molecular weight ($\overline{M}_n$), polydispersity index ($\overline{M}_w/\overline{M}_n$) of obtained copolymers.

Samples	$\overline{M}_w$	$\overline{M}_n$	$\overline{M}_w/\overline{M}_n$
Inulin	3942	3314	1.18
INU-Succ	5053	5007	1.19
INU-Succ-PEG	6665	5886	1.11

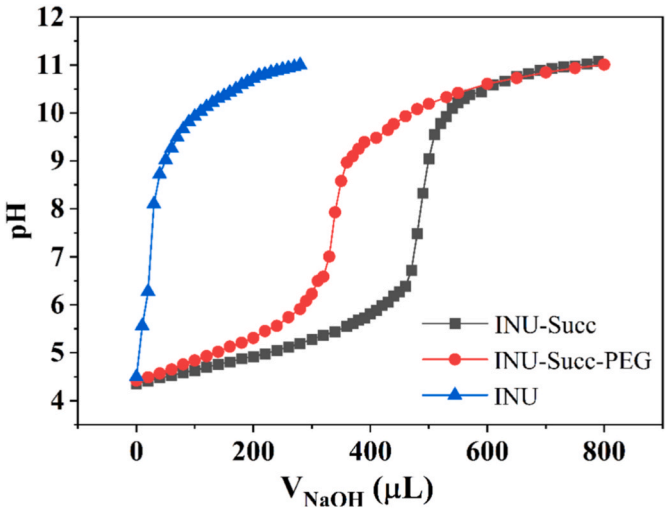

Fig. 2. Potentiometric titration curves of INU, INU-Succ, and INU-Succ-PEG copolymers.

and a complexation efficiency (CE), defined as the percentage of drug associated with the carrier relative to the initial used amount, close to quantitative values (100 ± 1.4 %), indicating that, under the selected conditions, all the Col was incorporated into the polyelectrolyte assemblies. This high incorporation efficiency highlights the strong affinity between the two components and confirms the robustness of the ionic complexation process, which also proved to be highly reproducible, being the mean values of DL and CE characterized by low standard deviation, obtained by repeating the reaction at least six times. The mildly acidic pH (6.5) was instrumental in promoting electrostatic interactions, ensuring that Col remained predominantly protonated while the carboxylic groups of INU-Succ-PEG were largely dissociated. AFM analysis (Fig. 3), performed to verify the successful formation of nanocomplexes and to investigate their morphological characteristics, showed that the INU-Succ-PEG/Col nanocomplexes had nanometric dimensions (approximately 2 nm) and a highly homogeneous size distribution. Stability studies in SLF using dynamic light scattering (DLS) confirmed the absence of aggregation of the complexes after 24 h incubation (data not shown).

Col is known to possess an intrinsic tendency to self-aggregate in aqueous media [37]. It was therefore of interest to investigate how its incorporation into INU-Succ-PEG/Col nanocomplexes modifies the self-aggregation ability of Col by using the pyrene assay [27]. Results, reported in Fig. 4 and expressed as the intensity ratio of the characteristic pyrene emission peaks in the presence of increasing amounts of either the nanocomplexes or free Col, show that incorporation of the drug in the nanocomplexes significantly alters its self-aggregation behaviour, showing a trend overlapping with that obtained for the copolymer alone. This effect clearly indicates the effective incorporation of the drug within the nanocomplexes formed with the copolymer through electrostatic interactions, leading to the formation of a supramolecular entity distinct from the free drug.

To further confirm the formation of a complex between Col and the copolymer, a ^{1}H NMR study was carried out. Fig. 5 shows the overlap of the ^{1}H NMR spectra of Col, INU-Succ-PEG, and the INU-Succ-PEG/Col complex in the range 3.3-0.4 δ, obtained under the selected experimental conditions. A comparison of the spectra clearly highlights changes in the proton resonances of Col in the presence of the copolymer [38,39]. In particular, the spectrum of the complex exhibits a pronounced line broadening of the peaks attributed to the -C**H**$_2$CH$_2$NH$_3^+$, -CH$_2$C**H**$_2$NH$_3^+$, (C**H**$_3$)$_2$CHCH$_2$-, (CH$_3$)$_2$C**H**CH$_2$- and (CH$_3$)$_2$CHC**H**$_2$- protons (δ ≈ 2.98, 2.20, 1.54, 1.09 and 0.71 ppm, respectively), indicating a modification in the peptide's chemical environment. This effect is consistent with the formation of a complex between Col and the

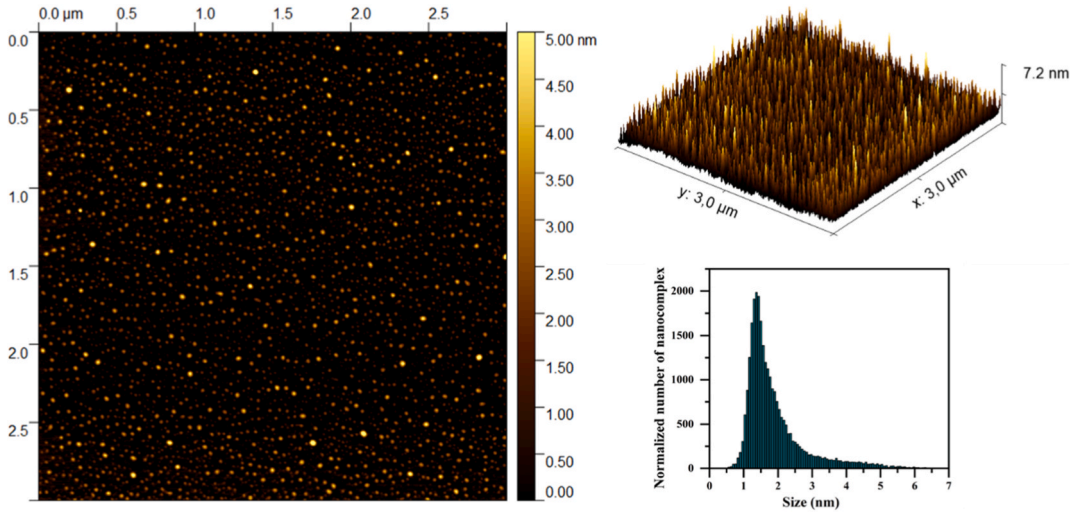

Fig. 3. Representative AFM 2D image, 3D reproduction, and dimensional analysis of INU-Succ-PEG/Col nanocomplexes.

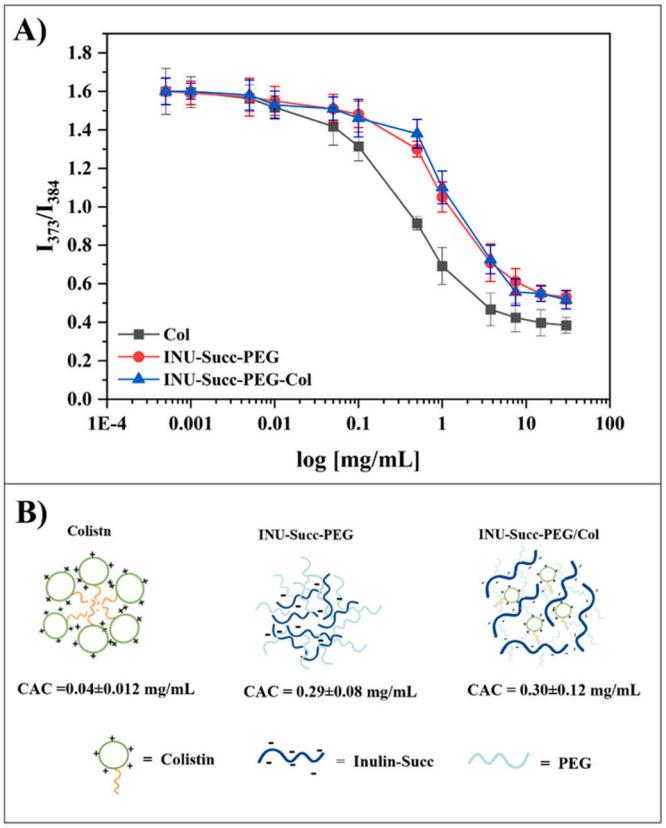

Fig. 4. (A) Plot of the intensity ratio I_{373}/I_{384} of pyrene fluorescence spectrum as a function of the aqueous concentration (log[mg/mL]) of Col, INU-Succ-PEG or INU-Succ-PEG/Col; (B) Schematic representation of the self-assembled systems.

copolymer: interactions with a macromolecular system reduce the molecular mobility of Col, resulting in broadened NMR signals [39].

With a view toward the development of an inhalable formulation, the aerodynamic behaviour of the Col/INU-Succ-PEG nanocomplex dispersions was evaluated and compared to Col alone using an Andersen Cascade Impactor (ACI). As shown in Fig. 6, the nebulization of both formulations produced aerosols characterized by very fine droplet sizes (below 2 µm) and a high fine particle fraction (FPF), exceeding 95%. Despite the comparable FPF values, relevant differences emerged in the deposition profile across the ACI stages. The INU-Succ-PEG/Col nanocomplexes showed a markedly higher deposition in stages 3–5 (≈57 % of nanocomplexes compared to ≈ 32 % of free Col), with a significant increase particularly at stage 5 (1.1 µm) compared to free Col. This aerodynamic range is generally considered optimal for deposition in the lower respiratory tract, suggesting a potentially improved targeting of the bronchial and bronchiolar regions. In contrast, free Col exhibited a distribution shifted toward the deepest impactor stages (stages 6–7, <0.7 µm) (≈37 % of free Col compared to ≈ 23 % of nanocomplexes), with significantly higher deposition at stage 7 (0.4 µm; $p < 0.001$). Particles in this ultrafine range are more susceptible to Brownian diffusion, which may reduce deposition efficiency in the distal lung and increase the likelihood of exhalation before reaching the target site. This behaviour is consistent with the smaller mass median aerodynamic diameter (MMAD) measured for free colistin (0.97 ± 0.08 µm) compared with INU-Succ-PEG/Col (1.27 ± 0.06 µm). Overall, INU-Succ-PEG/Col nanocomplexes significantly improved the aerodynamic behaviour of Col, promoting deposition within the optimal respirable window and highlighting their potential for efficient and targeted lung delivery via nebulization.

Since the nanocomplexes are designed for local pulmonary administration by nebulization, they will come into direct contact with the mucus layer lining the respiratory tract, which represents a critical physiological barrier to drug delivery. Mucus can hinder drug or particle diffusion through steric obstruction and adhesive interactions, potentially affecting the stability, aggregation behaviour, and transport of inhaled formulations. Therefore, a turbidimetric assay was performed to evaluate the capability of Col, in its free form or nanocomplexed, to interact with mucin by monitoring changes in dispersion turbidity upon mixing Col or Col-carrying nanocomplexes with mucin (Fig. 6a). Variations in turbidity may indicate strong interaction or the formation of aggregates. Conversely, limited changes in turbidity would suggest reduced mucoadhesive interactions, a desirable nanocomplex feature for efficient pulmonary delivery of Col.

As shown in Fig. 7A, clear differences in mucin interaction are observed among Col, the polymer, and the INU-Succ-PEG/Col nanocomplexes. In particular, Col alone causes a marked increase in turbidity, indicating strong interactions with mucin and suggesting the formation of aggregates within the mucus network. This behaviour suggests that free Col would be readily trapped in the mucus layer following in vivo local administration to the lungs. In contrast, the polymer alone shows little to no change in turbidity, indicating minimal interaction with mucin. The drug–polymer nanocomplexes display an

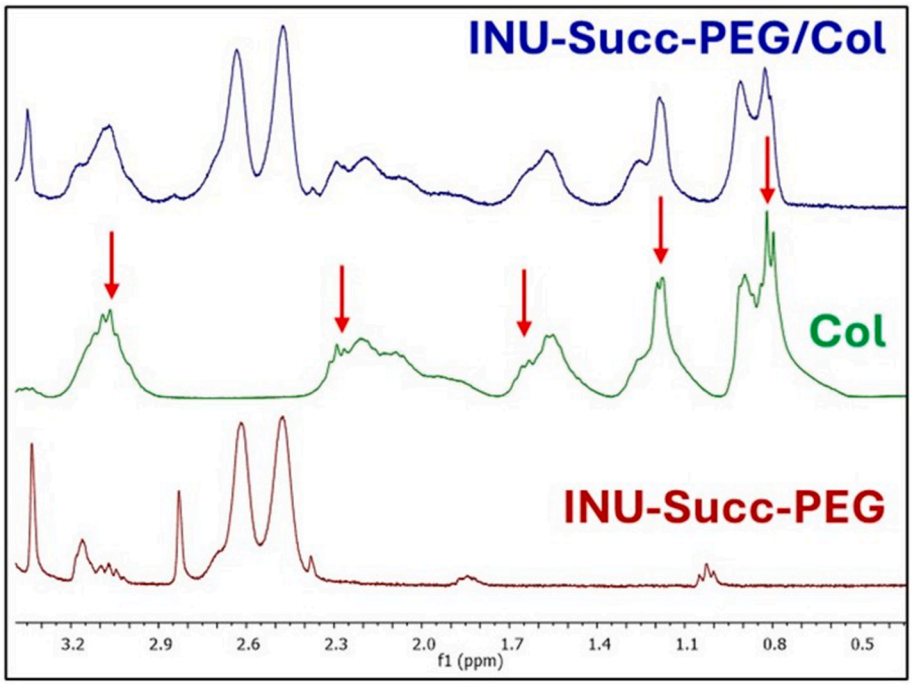

Fig. 5. Overlap of the ^{1}H NMR spectra of Col (green), INU-Succ-PEG (red) and INU-Succ-PEG/Col (blue) in the range 3.3-0.4 δ.

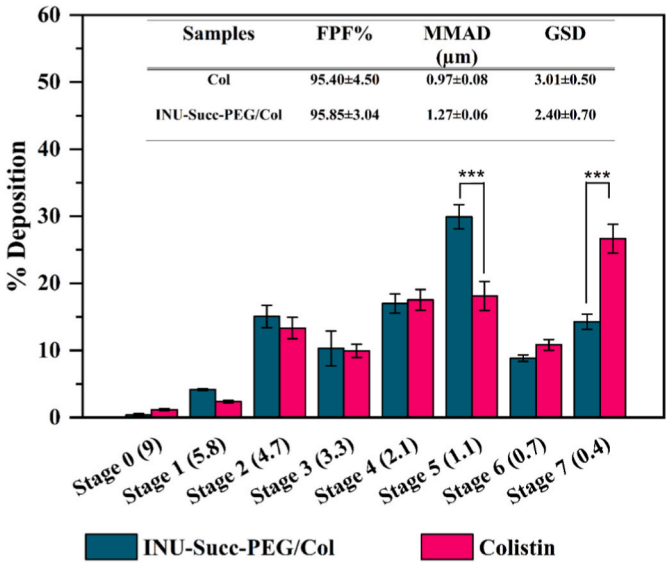

Fig. 6. Deposition of INU-Succ-PEG/Col nanocomplexes and Col alone aqueous dispersions after nebulization across the stages of ACI. Data are expressed as mean ± SD (n = 3). $p < 0.001$.

intermediate response, with a significantly lower turbidity increase compared to free Col, suggesting that complexation effectively limits Col–mucin binding, likely through partial shielding of charged groups. Moreover, to evaluate the ability of the nanocomplexes to cross the mucus layer, a muco-diffusion test was carried out. Results (Fig. 7B) demonstrate that Col-carrying nanocomplex diffuses through the mucus barrier, while free Col is trapped within the mucus layer. Such results are critical to demonstrate that the INU-Succ-PEG/Col nanocomplexes can deliver the drug efficiently to the lower respiratory tract without being hindered by mucin interactions.

Since the potential diffusion/entrapment of the drug within the mucus layer may depend on the dissociation of the nanocomplex and therefore, from the drug release in the presence of mucin, a drug release study was carried out in PBS, both in the absence and in the presence of mucin, by using the dialysis method. In addition, to better mimic the pulmonary environment, the same study was performed in SLF. As shown in Fig. 8B, free Col diffuses rapidly through the dialysis membrane in both PBS and SLF at pH 7.4. In contrast, its diffusion is drastically slowed in the presence of mucin, confirming strong interactions between free Col and the mucin network (Fig. 8A). In contrast to free Col, the release behaviour of INU-Succ-PEG/Col nanocomplexes was moderately influenced by the release medium. A significantly higher amount of Col was released in SLF compared to PBS during the first 4 h ($p < 0.05$), indicating an enhanced early-phase release under simulated lung conditions. However, beyond this initial phase, the release profiles in the two media became comparable. Notably, the presence of mucin did not significantly affect Col release from the nanocomplexes, suggesting that drug liberation is primarily governed by nanocomplex dissociation rather than by specific drug–mucin interactions.

Importantly, the cumulative amount of Col released remained below approximately 60 wt% within the first 6 h in all tested conditions, confirming a sustained and controlled release profile. Overall, these findings support the ability of the nanocomplexes to mitigate Col interactions with the mucus network while enabling controlled drug release, thereby reducing premature drug diffusion and potential entrapment within the mucus layer.

3.3. *In vitro biological performances of Col-carrying nanocomplexes*

After demonstrating the ability of nanocomplexes to diffuse through the mucus and release Col in a controlled manner, with no influence of mucin on the release kinetics, the biological effects of the system were subsequently evaluated. In particular, the impact was assessed on bronchial epithelial cells to investigate biocompatibility, and on Gram-negative bacteria commonly found in the lungs of patients with inflammatory pulmonary diseases. Among these pathogens, *K. pneumoniae* represents a major causative agent of respiratory infections. In addition, *E. coli*, although less prevalent, is a Gram-negative bacterium that can colonize the respiratory tract of cystic fibrosis (CF) patients, particularly during specific stages of the disease or during pulmonary exacerbations, contributing to chronic inflammation [2].

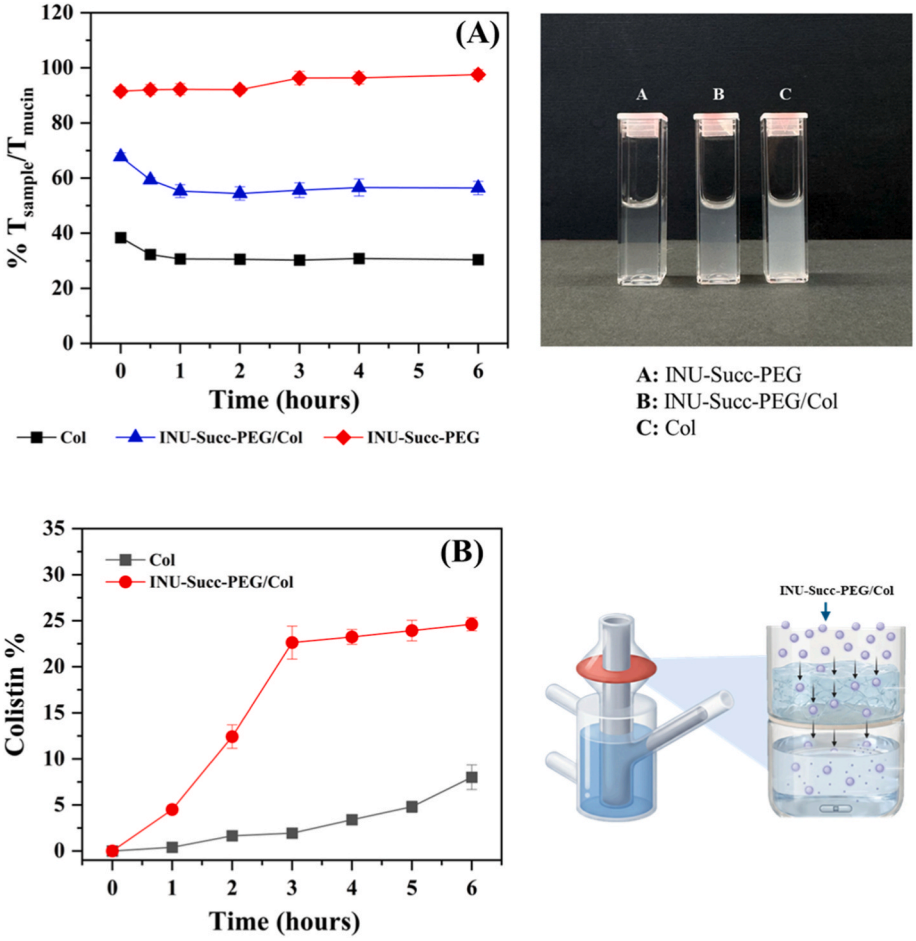

Fig. 7. (A) Turbidity of mucin aqueous dispersions (1 mg/mL) in the presence of Col, INU-Succ-PEG or INU-Succ-PEG/Col (left), expressed as transmittance ratio % at λ = 500 nm (data reported as means SD, n = 3), and appearance of the dispersions before analysis (right); (B) muco-diffusion test expressed as Col diffusion % (left), evaluated by Frantz cell (right).

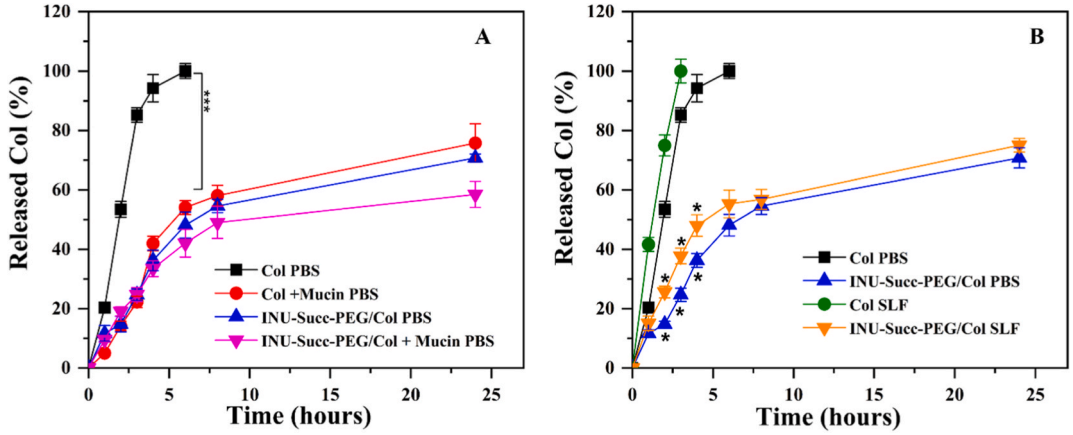

Fig. 8. Release profile of Col from INU-Succ-PEG/Col nanocomplex, expressed as % of released Col as a function of incubation time at 37 °C, compared to the Col diffusion through the dialysis membrane in (A) PBS/mucin and (B) SLF (***p < 0.001).

Cell viability tests were performed on two pulmonary cell lines, BEAS-2B and 16HBE, which were selected because they are well-established in vitro models of human bronchial epithelial cells and are widely used to study respiratory toxicity and lung-related biological responses [40]. The results, reported in Fig. 9A–B for BEAS and 16HBE, respectively, showed the absence of cytotoxic effects within the tested concentration range in both cell lines.

Antibacterial activity was evaluated using colistimethate sodium (CMS), the clinically approved prodrug of Col, as a reference. Although native Col exhibits potent antibacterial activity, its direct clinical use is limited by severe systemic toxicity, including nephrotoxicity and neurotoxicity, as well as respiratory adverse effects upon inhalation. Consequently, Col is administered as CMS, a less toxic prodrug that undergoes in vivo conversion to the active form. However, this

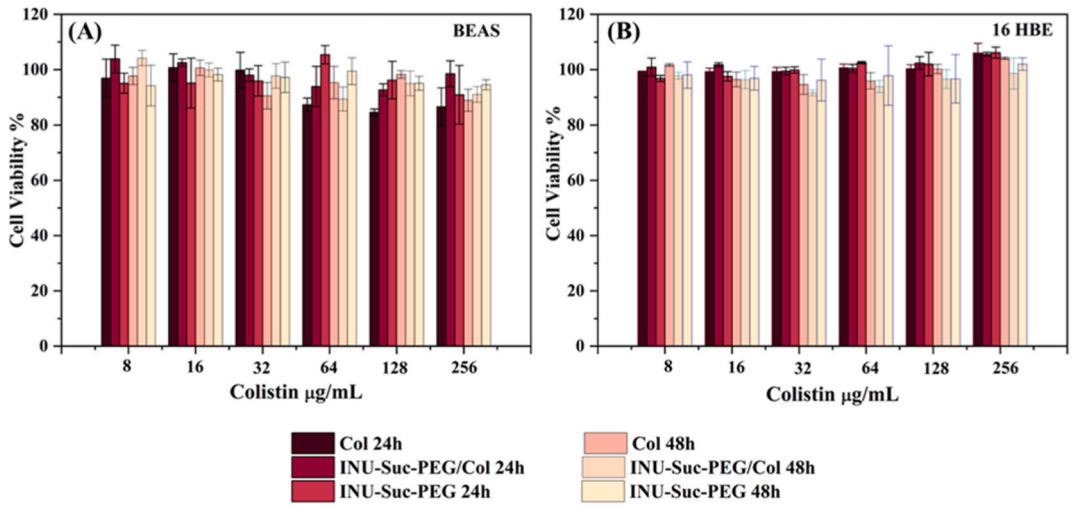

Fig. 9. Cell viability of Col and INU-Succ-PEG/Col nanocomplexes, and INU-Succ-PEG copolymer on BEAS (A) and 16-HBE (B) cell lines, after 24 and 48 h of incubation.

conversion process is often incomplete and variable, leading to unpredictable and sometimes subtherapeutic drug concentrations in lung tissue and plasma, which may compromise efficacy and promote the development of bacterial resistance [41]. Antibacterial tests, performed on Gram-negative strains *K. pneumoniae* and *E. coli*, reported in Fig. 10A–B, showed that the copolymer alone did not exhibit any antimicrobial activity, whereas the nanocomplex with colistin displayed clear antimicrobial efficacy.

Both MIC and IC_{50} values (Table 2) were significantly lower than that of the clinically used prodrug CMS, indicating substantially improved antibacterial potency. This finding is particularly relevant given that native Col is not used clinically due to toxicity concerns. While further investigation is required, these findings suggest that nanocomplexation may represent a promising approach to enhance the local pulmonary delivery of Col.

From a therapeutic perspective, the efficient pulmonary deposition, combined with the sustained release profile and the reduced interaction with mucus observed for the INU-Succ-PEG/Col nanocomplexes, may enable higher local drug concentrations at the site of infection while minimizing systemic exposure. This could translate into improved efficacy against persistent Gram-negative lung infections, reduced dosing frequency, and a lower risk of toxicity, addressing key limitations of current colistin-based therapies and offering a promising strategy for the treatment of chronic pulmonary bacterial infections. This could be particularly relevant in the context of CF, where chronic lung infections caused by Gram-negative pathogens are sustained by thick mucus, biofilm formation, and limited antibiotic penetration.

4. Conclusion

The present work describes the successful development of a negatively charged INU-based graft copolymer designed to form nanocomplexes with Col and improve its pulmonary delivery. The synthetic strategy proved to be highly controllable and reproducible, enabling modulation of the polymer charge density and subsequent PEG functionalization, while preserving favourable physicochemical properties such as aqueous solubility and low polydispersity. The presence of ionizable carboxyl groups, even after PEGylation, ensured effective electrostatic interaction with the cationic drug and the formation of stable supramolecular nanocomplexes. At the nanoscale, the polymer–drug system formed homogeneous nanocomplexes and significantly modified the intrinsic aggregation behaviour of Col in aqueous media, confirming successful complexation. After aqueous dispersion, the favourable aerodynamic behaviour observed after nebulization supports the feasibility of efficient lung deposition. The most relevant findings concern the interaction with mucus and muco-diffusion: free Col exhibited a marked tendency to interact with mucin, a behaviour that may limit its diffusion through the mucus layer and potentially reduce the fraction of drug reaching the site of infection after inhalation. In contrast, complexation with the polymer reduced these interactions allowing muco-diffusion, likely due to partial shielding of the drug's charged groups. This feature is particularly advantageous in the context of chronic pulmonary diseases, where thickened mucus represents a major barrier to effective antibiotic therapy. Release studies further demonstrated that the nanocomplexes provide a controlled and sustained drug release profile, that was not significantly influenced by the presence of mucin. This suggests that the Col involved in the complex formation is less susceptible to premature drug sequestration within the mucus network compared to free Col. Such controlled release behaviour may contribute to maintaining therapeutic concentrations at the infection site for prolonged periods, potentially reducing dosing frequency and minimizing peak-related toxicity. Importantly, the copolymer showed excellent biocompatibility toward bronchial epithelial cells, confirming its suitability for pulmonary administration. Moreover, the antibacterial activity of Col was fully preserved after complexation, indicating that the polymer carrier does not impair the intrinsic antimicrobial efficacy of the drug. This is a crucial aspect, as native Col, although highly potent, is associated with significant systemic and pulmonary toxicity, while its clinically used prodrug may lead to suboptimal and variable drug levels. The polymer-based system therefore represents a strategy to combine the high efficacy of Col with improved control over its local delivery and exposure.

Overall, compared with the administration of colistin alone, the INU-Succ-PEG/Col nanocomplexes offer multifunctional advantages: improved interaction with the pulmonary environment, controlled release, preserved antibacterial activity, and good biocompatibility. These findings highlight the potential of this nanotechnological platform as a promising alternative approach for the treatment of chronic Gram-negative lung infections, particularly in conditions characterized by impaired mucus clearance.

Funding

The research leading to these results has received funding from the European Union - NextGenerationEU through the Italian Ministry of University and Research under PNRR - M4C2-I1.3 Project PE_00000019: " Health Extended Alliance for Innovative Therapies, Advanced Lab-research, and Integrated Approaches of Precision Medicine - HEAL

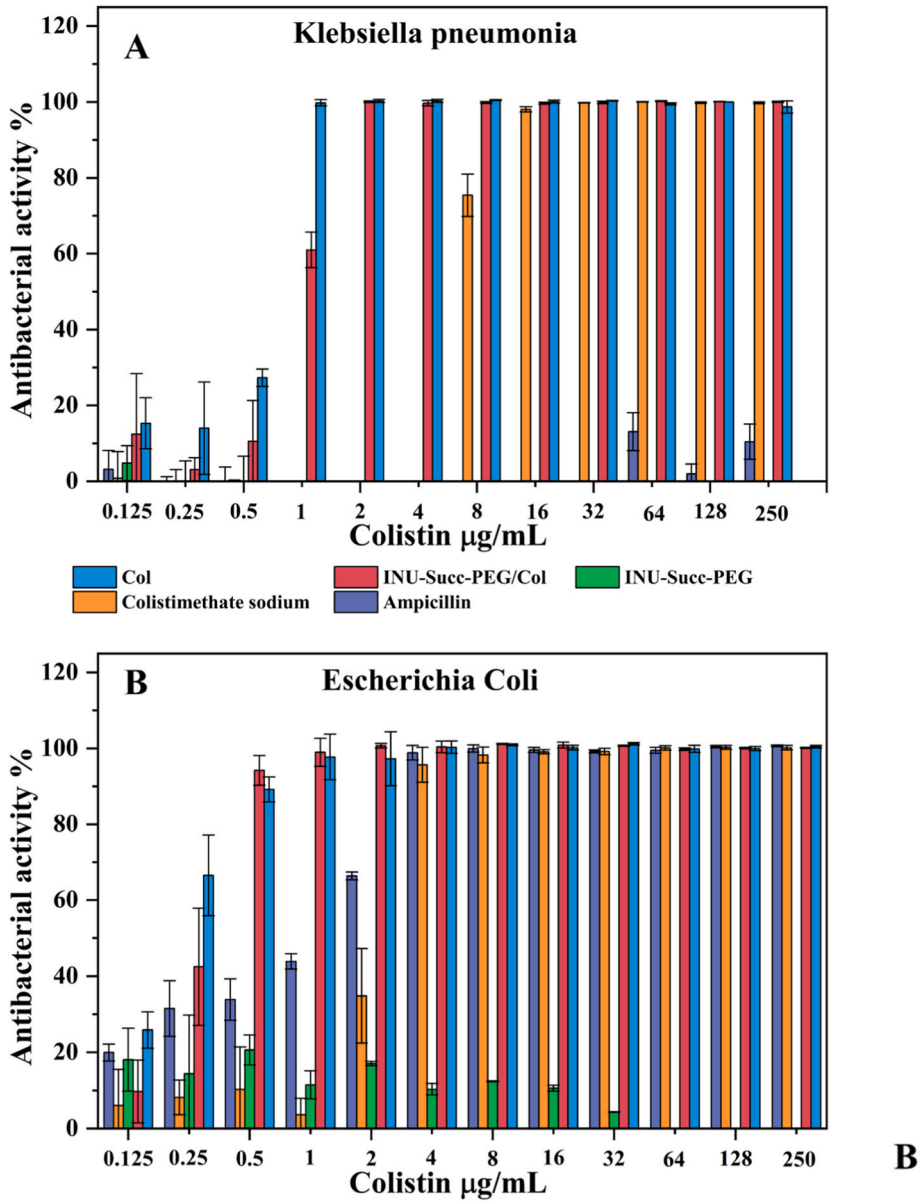

Fig. 10. Antibacterial activity % of Col and INU-Succ-PEG/Col nanocomplexes and on *K. pneumoniae* (A) and *E. coli* (B). CMS sodium, INU-Succ-PEG copolymer and Ampicillin were used as controls.

Table 2
In vitro antibacterial activity expressed as the MIC and the half-maximal inhibitory concentration (IC50) values.

Sample	*K. pneumoniae*		*E. coli*	
	MIC (µg/ml)	IC50 (µg/ml)	MIC (µg/ml)	IC50 (µg/ml)
Ampicillin	>256	n.a.	4	1.7
CMS	16	6.9	4	2.4
Col	1	0.58	1	0.23
INU-Succ-PEG/Col	2	1.05	1	0.30
INU-Succ-PEG	>256	n.a.	>256	n.a.

ITALIA" to Gennara Cavallaro. CUP: B73C22001250006. The views and opinions expressed are those of the authors only and do not necessarily reflect those of the European Union or the European Commission. Neither the European Union nor the European Commission can be held responsible for them.

CRediT authorship contribution statement

Cinzia Scialabba: Data curation, Formal analysis, Writing – original draft. **Nina Bono:** Formal analysis, Investigation. **Salvatore Emanuele Drago:** Formal analysis, Investigation. **Francesca Terracina:** Formal analysis, Investigation. **Paolo Tarsini:** Formal analysis, Investigation. **Emanuela Fabiola Craparo:** Conceptualization, Methodology, Writing – original draft. **Gabriele Candiani:** Formal analysis, Investigation. **Gennara Cavallaro:** Conceptualization, Supervision, Writing – review & editing.

Declaration of competing interest

The authors declare that they have no known competing financial interests or personal relationships that could have appeared to influence the work reported in this paper.

Data availability

Data will be made available on request.

References

[1] X. Bian, X. Qu, J. Zhang, S.C. Nang, P.J. Bergen, Q. Tony Zhou, H.K. Chan, M. Feng, J. Li, Pharmacokinetics and pharmacodynamics of peptide antibiotics, Adv. Drug Deliv. Rev. 183 (2022), https://doi.org/10.1016/j.addr.2022.114171.

[2] S. Malhotra, D. Hayes, D.J. Wozniak, Cystic Fibrosis and Pseudomonas Aeruginosa: the Host-Microbe Interface, 2019.

[3] M.U. Ahmed, T. Velkov, Y.W. Lin, B. Yun, C.J. Nowell, F. Zhou, Q.T. Zhou, K. Chan, M.A.K. Azad, J. Li, Potential toxicity of polymyxins in human lung epithelial cells, Antimicrob. Agents Chemother. 61 (2017), https://doi.org/10.1128/AAC.02690-16.

[4] G.A. Alothman, B. Ho, M.M. Alsaadi, S.L. Ho, L. O'Drowsky, E. Louca, A.L. Coates, Bronchial constriction and inhaled colistin in cystic fibrosis, Chest 127 (2005) 522–529, https://doi.org/10.1378/chest.127.2.522.

[5] E.M. Westerman, P.P.H. Le Brun, D.J. Touw, H.W. Frijlink, H.G.M. Heijerman, Effect of nebulized colistin sulphate and colistin sulphomethate on lung function in patients with cystic fibrosis: a pilot study, J. Cyst. Fibros. 3 (2004) 23–28, https://doi.org/10.1016/j.jcf.2003.12.005.

[6] Y. Wang, R.Y.K. Chang, W.J. Britton, H.K. Chan, Advances in the development of antimicrobial peptides and proteins for inhaled therapy, Adv. Drug Deliv. Rev. 180 (2022), https://doi.org/10.1016/j.addr.2021.114066.

[7] N. Grégoire, V. Aranzana-Climent, S. Magréault, S. Marchand, W. Couet, Clinical pharmacokinetics and pharmacodynamics of Colistin, Clin. Pharmacokinet. 56 (2017) 1441–1460, https://doi.org/10.1007/s40262-017-0561-1.

[8] R. Imberti, M. Cusato, P. Villani, L. Carnevale, G.A. Iotti, M. Langer, M. Regazzi, Steady-state pharmacokinetics and BAL concentration of colistin in critically ill patients after IV colistin methanesulfonate administration, Chest 138 (2010) 1333–1339, https://doi.org/10.1378/chest.10-0463.

[9] N. Narimisa, A. Keshtkar, L. Dadgar-Zankbar, N. Bostanghadiri, Y.R. Far, S. Shahroodian, A. Zahedi Bialvaei, S. Razavi, Prevalence of colistin resistance in clinical isolates of Pseudomonas aeruginosa: a systematic review and meta-analysis, Front. Microbiol. 15 (2024), https://doi.org/10.3389/fmicb.2024.1477836.

[10] C. Zhu, E.K. Schneider, J. Wang, K. Kempe, P. Wilson, T. Velkov, J. Li, T.P. Davis, M.R. Whittaker, D.M. Haddleton, A traceless reversible polymeric colistin prodrug to combat multidrug-resistant (MDR) gram-negative bacteria, J. Contr. Release 259 (2017) 83–91, https://doi.org/10.1016/j.jconrel.2017.02.005.

[11] Y. Li, C. Tang, E. Zhang, L. Yang, Colistin-entrapped liposomes driven by the electrostatic interaction: mechanism of drug loading and in vivo characterization, Int. J. Pharm. 515 (2016) 20–29, https://doi.org/10.1016/j.ijpharm.2016.10.001.

[12] S. Yu, S. Wang, P. Zou, G. Chai, Y.W. Lin, T. Velkov, J. Li, W. Pan, Q.T. Zhou, Inhalable liposomal powder formulations for co-delivery of synergistic ciprofloxacin and colistin against multi-drug resistant gram-negative lung infections, Int. J. Pharm. 575 (2020), https://doi.org/10.1016/j.ijpharm.2019.118915.

[13] S. Yu, H. Yuan, G. Chai, K. Peng, P. Zou, X. Li, J. Li, F. Zhou, H.K. Chan, Q.T. Zhou, Optimization of inhalable liposomal powder formulations and evaluation of their in vitro drug delivery behavior in Calu-3 human lung epithelial cells, Int. J. Pharm. 586 (2020), https://doi.org/10.1016/j.ijpharm.2020.119570.

[14] G. Landa, T. Alejo, T. Sauzet, J. Laroche, V. Sebastian, F. Tewes, M. Arruebo, Colistin-loaded aerosolizable particles for the treatment of bacterial respiratory infections, Int. J. Pharm. 635 (2023), https://doi.org/10.1016/j.ijpharm.2023.122732.

[15] M. Pastor, M. Moreno-Sastre, A. Esquisabel, E. Sans, M. Viñas, D. Bachiller, V. J. Asensio, Á. Del Pozo, E. Gainza, J.L. Pedraz, Sodium colistimethate loaded lipid nanocarriers for the treatment of Pseudomonas aeruginosa infections associated with cystic fibrosis, Int. J. Pharm. 477 (2014) 485–494, https://doi.org/10.1016/j.ijpharm.2014.10.048.

[16] S. Yu, X. Pu, M.U. Ahmed, H.H. Yu, T.T. Mutukuri, J. Li, Q.T. Zhou, Spray-freeze-dried inhalable composite microparticles containing nanoparticles of combinational drugs for potential treatment of lung infections caused by Pseudomonas aeruginosa, Int. J. Pharm. 610 (2021), https://doi.org/10.1016/j.ijpharm.2021.121160.

[17] G. Bakirdogen, E. Selcuk, E.L. Sahkulubey Kahveci, T. Ozbek, S. Derman, M. U. Kahveci, Fabrication of poly(β-amino ester) and hyaluronic acid based pH responsive nanocomplex as an antibiotic release system, Int. J. Biol. Macromol. 258 (2024), https://doi.org/10.1016/j.ijbiomac.2023.129060.

[18] N.V. Dubashynskaya, S.V. Raik, Y.A. Dubrovskii, E.S. Shcherbakova, E. V. Demyanova, A.Y. Shasherina, Y.A. Anufrikov, D.N. Poshina, A.V. Dobrodumov, Y.A. Skorik, Hyaluronan/colistin polyelectrolyte complexes: promising antiinfective drug delivery systems, Int. J. Biol. Macromol. 187 (2021) 157–165, https://doi.org/10.1016/j.ijbiomac.2021.07.114.

[19] T.D. Vogelaar, A.E. Agger, J.E. Reseland, D. Linke, H. Jenssen, R. Lund, Crafting stable antibiotic nanoparticles via complex coacervation of colistin with block copolymers, Biomacromolecules 25 (2024) 4267–4280, https://doi.org/10.1021/acs.biomac.4c00337.

[20] M.A. Mensink, H.W. Frijlink, K. Van Der Voort Maarschalk, W.L.J. Hinrichs, Inulin, a flexible oligosaccharide. II: review of its pharmaceutical applications, Carbohydr. Polym. 134 (2015) 418–428, https://doi.org/10.1016/j.carbpol.2015.08.022.

[21] A. Franck, Technological functionality of inulin and oligofructose, Br. J. Nutr. 87 (2002) S287–S291, https://doi.org/10.1079/bjn/2002550.

[22] C.V. Stevens, A. Meriggi, K. Booten, Chemical modification of inulin, a valuable renewable resource, and its industrial applications, Biomacromolecules 2 (2001) 1–16, https://doi.org/10.1021/bm005642t.

[23] L. Catenacci, M. Sorrenti, S. Perteghella, D. Mandracchia, M.L. Torre, A. Trapani, C. Milanese, G. Tripodo, Combination of inulin and β-cyclodextrin properties for colon delivery of hydrophobic drugs, Int. J. Pharm. 589 (2020), https://doi.org/10.1016/j.ijpharm.2020.119861.

[24] G. Rassu, B. Pavan, D. Mandracchia, G. Tripodo, G. Botti, A. Dalpiaz, E. Gavini, P. Giunchedi, Polymeric nanomicelles based on inulin D α-tocopherol succinate for the treatment of diabetic retinopathy, J. Drug Deliv. Sci. Technol. 61 (2021), https://doi.org/10.1016/j.jddst.2020.102286.

[25] C. Sardo, E.F. Craparo, B. Porsio, G. Giammona, G. Cavallaro, Improvements in rational design strategies of inulin derivative polycation for siRNA delivery, Biomacromolecules 17 (2016) 2352–2366, https://doi.org/10.1021/acs.biomac.6b00281.

[26] M.R.C. Marques, R. Loebenberg, M. Almukainzi, Simulated biological fluids with possible application in dissolution testing, Dissolut. Technol 18 (2011) 15–28, https://doi.org/10.14227/DT180311P15.

[27] D. Triolo, E.F. Craparo, B. Porsio, C. Fiorica, G. Giammona, G. Cavallaro, Polymeric drug delivery micelle-like nanocarriers for pulmonary administration of beclomethasone dipropionate, Colloids Surf. B Biointerfaces 151 (2017) 206–214, https://doi.org/10.1016/j.colsurfb.2016.11.025.

[28] S.E. Drago, M. Cabibbo, C. Scialabba, E.F. Craparo, G. Cavallaro, Smart inhalation therapy: boosting siRNA efficacy with inulin-based multifunctional polymers, ACS Appl. Mater. Interfaces 17 (2025) 62647–62661, https://doi.org/10.1021/acsami.5c18977.

[29] S. Yadav, M. Mahato, R. Pathak, D. Jha, B. Kumar, S.R. Deka, H.K. Gautam, A. K. Sharma, Multifunctional self-assembled cationic peptide nanostructures efficiently carry plasmid DNA in vitro and exhibit antimicrobial activity with minimal toxicity, J. Mater. Chem. B 2 (2014) 4848–4861, https://doi.org/10.1039/C4TB00657G.

[30] C. Pennetta, N. Bono, F. Ponti, M.C. Bellucci, F. Viani, G. Candiani, A. Volonterio, Multifunctional neomycin-triazine-based cationic lipids for gene delivery with antibacterial properties, Bioconjug. Chem. 32 (2021) 690–701, https://doi.org/10.1021/acs.bioconjchem.0c00616.

[31] Y. Hu, L. Liu, X. Zhang, Y. Feng, Z. Zong, In vitro activity of Neomycin, Streptomycin, Paromomycin and Apramycin against carbapenem-resistant Enterobacteriaceae clinical strains, Front. Microbiol. 8 (2017), https://doi.org/10.3389/fmicb.2017.02275, 2017.

[32] G. Cavallaro, C. Sardo, C. Scialabba, M. Licciardi, G. Giammona, Smart Inulin-based Polycationic Nanodevices for Sirna Delivery, 2017.

[33] E.F. Craparo, S.E. Drago, F. Quaglia, F. Ungaro, G. Cavallaro, Development of a novel rapamycin loaded nano- into micro-formulation for treatment of lung inflammation, Drug Deliv. Transl. Res. 12 (2022) 1859–1872, https://doi.org/10.1007/s13346-021-01102-5.

[34] M. El Batouti, W. Sadik, A.G. Eldemerdash, E. Hanafy, H.A. Fetouh, New and innovative microwave-assisted technology for synthesis of guar gum-grafted acrylamide hydrogel superabsorbent for the removal of acid red 8 dye from industrial wastewater, Polym. Bull. 80 (2023) 4965–4989, https://doi.org/10.1007/s00289-022-04254-7.

[35] S. Chami, N. Joly, P. Bocchetta, P. Martin, D. Aliouche, Polyacrylamide grafted Xanthan: microwave-assisted synthesis and rheological behavior for polymer flooding, Polymers 13 (2021) 1484, https://doi.org/10.3390/polym13091484.

[36] E.F. Craparo, T. Musumeci, A. Bonaccorso, R. Pellitteri, A. Romeo, I. Naletova, L. M. Cucci, G. Cavallaro, C. Satriano, Mpeg-plga nanoparticles labelled with loaded or conjugated rhodamine-b for potential nose-to-brain delivery, Pharmaceutics 13 (2021), https://doi.org/10.3390/pharmaceutics13091508.

[37] S.J. Wallace, J. Li, R.L. Nation, R.J. Prankerd, T. Velkov, B.J. Boyd, Self-assembly behavior of colistin and its prodrug colistin methanesulfonate: implications for solution stability and solubilization, J. Phys. Chem. B 114 (2010) 4836–4840, https://doi.org/10.1021/jp100458x.

[38] M.A. Khumaini Mudhar Bintang, V. Tipmanee, T. Srichana, Colistin sulfate-sodium deoxycholate sulfate micelle formulations; molecular interactions, cell nephrotoxicity and bioactivity, J. Drug Deliv. Sci. Technol. 79 (2023), https://doi.org/10.1016/j.jddst.2022.104091.

[39] F.A. Gogry, M.T. Siddiqui, I. Sultan, F.M. Husain, A.A. Al-Kheraif, A. Ali, Q. M. Rizwanul Haq, Colistin interaction and surface changes associated with mcr-1 conferred plasmid mediated resistance in E. coli and A. veronii strains, Pharmaceutics 14 (2022), https://doi.org/10.3390/pharmaceutics14020295.

[40] M. Zhang, C. Hu, G. Yang, Y. Hu, Y. Qu, Cytoprotective role of resveratrol in cigarette smoke-induced pyroptosis through Nrf2 pathway activation, Cell Stress Chaperones 30 (2025), https://doi.org/10.1016/j.cstres.2025.100107.

[41] P.J. Zamri, S.M.S. Lim, F.B. Sime, J.A. Roberts, M.H. Abdul-Aziz, A systematic review of pharmacokinetic studies of colistin and polymyxin B in adult populations, Clin. Pharmacokinet. 64 (2025) 655–689, https://doi.org/10.1007/s40262-025-01488-2.